inorganics

MDPI

Article

Flux Synthesis, Crystal Structures, and Magnetism of the Series $La_{2n+2}MnSe_{n+2}O_{2n+2}$ (n = 0–2)

Simon Peschke and Dirk Johrendt *

Department Chemie, Ludwig-Maximilians-Universität München, Butenandtstr. 5-13 (D), 81377 München, Germany; simon.peschke@cup.uni-muenchen.de

* Correspondence: johrendt@lmu.de; Tel.: +49-89-2180-77430

Academic Editor: Duncan H. Gregory

Received: 19 December 2016; Accepted: 15 January 2017; Published: 31 January 2017

Abstract: Three members of the homologous series of manganese oxyselenides with the general formula $La_{2n+2}MnSe_{n+2}O_{2n+2}$ (n = 0–2) have been synthesized in a NaI/KI flux and characterized by single-crystal X-ray diffraction, powder X-ray diffraction and magnetic measurements. The structures consist of chains of edge-sharing $MnSe_4O_2$-octahedra along the b-axis which are linked together along the a-axis by edge-sharing OLa_4- and/or OLa_3Mn-tetrahedra forming infinite ribbons of increasing width. mC-$La_2MnSe_2O_2$ ($Pb_2HgCl_2O_2$-type, $C2/m$, a = 11.6621(5) Å, b = 3.9719(1) Å, c = 7.2049(3) Å, β = 121.655(2)°) represents a new polymorph of this compound. $La_4MnSe_3O_4$ ($P2/m$, a = 9.0055(4) Å, b = 4.0186(1) Å, c = 7.1946(3) Å, β = 109.715(2)°) and $La_6MnSe_4O_6$ ($C2/m$, a = 24.760(2) Å, b = 4.0359(3) Å, c = 7.1850(6) Å, β = 104.162(3)°) exhibit new structure types. Magnetic measurements suggest antiferromagnetic order of the moments below about 15 K with effective magnetic moments of 5.53(1), 5.99(1) and 6.01(1) μ_B per formula unit for n = 1, 2 and 3, respectively.

Keywords: manganese; rare-earth; oxyselenides; crystal structure; magnetism

1. Introduction

The research into structural chemistry and physical properties of transition-metal oxyselenides has been very fruitful during the last years. Numerous new compounds with the general formula $RE_2TSe_2O_2$ (RE = La, Ce; T = Cd, Fe, Mn, Zn) [1–9] have been discovered and their structures and magnetism have been studied. Among the particular families, different polymorphs may exist which makes the diversity even bigger. In order to distinguish the different polymorphs mentioned in this paper, we extend the formulae by the *Pearson* letters. Recently, we found new polymorphs in the $RE_2FeSe_2O_2$-family (RE = La, Ce) [2]. mC-$La_2FeSe_2O_2$ and mC-$Ce_2FeSe_2O_2$ crystallize in the $Pb_2HgCl_2O_2$-structure type with distorted edge-sharing $FeSe_4O_2$-octahedra linked together by edge-sharing OLa_3Fe-tetrahedra forming infinite ribbons which are two tetrahedra in width. Similar building blocks with an analogous connectivity between the TSe_4O_2-octahedra and the ORE_3T-tetrahedra have already been observed in the compounds $RE_{3.67}Ti_2Se_6O_3$ (RE = Ce, Nd, Sm) [10], $La_4Ti_2Se_5O_4$ [11], $La_6Ti_3Se_9O_5$ [11] and $CeCrSe_2O$ [12]. Beside the iron compounds, there are two polymorphs known in the analogous manganese family. oC-$La_2MnSe_2O_2$ [1] has a defect ZrCuSiAs-type structure with slabs of edge-sharing OLa_4-tetrahedra stacked alternating with slabs of $MnSe_4$-tetrahedra. The structure of oA-$La_2MnSe_2O_2$ [8] consists of $MnSe_4$-tetrahedra and edge-sharing $MnSe_4O_2$-octahedra which are connected by infinite ribbons of edge-sharing OLa_4- and OLa_3Mn-tetrahedra four units wide.

Beside oxyselenides with the general chemical composition above, numerous other rare-earth oxyselenides are known, for example $RE_4TiSe_4O_4$ (RE = Sm, Gd, Tb, Dy, Ho, Er, Y) [13,14] and $RE_4O_4Se(Se_2)$ (RE = La, Ce, Pr, Nd, Sm) [15]. $RE_4TiSe_4O_4$ can be regarded as a defect variant of oA-$La_2MnSe_2O_2$ with the same building blocks but without $TiSe_4$-tetrahedra. In contrast, $RE_4O_4Se(Se_2)$

compounds contain Se^{2-} anions as well as $(Se-Se)^{2-}$ dumbbells, which are separated by layers of distorted $(RE_4O)^{10+}$ tetrahedra. Their magnetism origins from the $4f$-electrons of the particular rare-earth metal, and spin frustration is observed in the rare-earth-oxide tetrahedra of these compounds [15]. Formally, it should be possible to insert divalent transition-metals in this structure by breaking up the diselenide units leading to the formula $RE_4TSe_3O_4$.

In this paper, we present $La_4MnSe_3O_4$ as the first example of such compounds with only Se^{2-} anions in a new structure related to the $RE_4TiSe_4O_4$-type. $La_4MnSe_3O_4$ can formally be obtained by adding one La_2SeO_2-unit to $La_2MnSe_2O_2$. We were also successful to add a second La_2SeO_2-unit in order to obtain the compound $La_6MnSe_4O_6$, which represents the third member of the homologous series $La_{2n+2}MnSe_{n+2}O_{2n+2}$. Additional we have found mC-$La_2MnSe_2O_2$ as a new polymorph to the manganese-family and present magnetic susceptibility data of all compounds.

2. Results

Since conventional solid state synthesis did not lead to satisfying results, a flux synthesis was developed in order to get high purity samples (>95 wt %). mC-$La_2MnSe_2O_2$ was synthesized in a NaI/KI-flux at 1273 K starting from the low temperature polymorph oC-$La_2MnSe_2O_2$. The other two members of the homologous series were synthesized starting from the binary compounds La_2O_3, La_2Se_3 and MnSe, which were pre-reacted at 873 K, homogenized and then heated in a NaI/KI-flux at 1273–1373 K. After washing the reaction mixture to remove the flux, a large amount of bright brown, transparent rod-like crystals, as well as polycrystalline yellow-brown powders were obtained. The crystal structures were determined by single-crystal X-ray diffraction. A comparison of the obtained data is given in Table 1, for details see Tables A1–A3 in the appendix. mC-$La_2MnSe_2O_2$ and $La_6MnSe_4O_6$ adopt monoclinic $C2/m$ (No. 12) symmetry, whereas $La_4MnSe_3O_4$ crystallizes in space group $P2/m$ (No. 10). It is noticeable, that the lattice parameter b increases (≈1.6%) and c decreases (≈0.3%) slightly with increasing n. In contrast, the monoclinic angle β decreases strongly (≈14%) with increasing n. Further relevant crystallographic data are compiled in the appendix.

Table 1. Crystal data and structure refinement of $La_{2n+2}MnSe_{n+2}O_{2n+2}$ (n = 0, 1, 2).

	mC-$La_2MnSe_2O_2$	$La_4MnSe_3O_4$	$La_6MnSe_4O_6$
Space group	$C2/m$	$P2/m$	$C2/m$
a (Å)	11.6621(5)	9.0055(4)	24.760(2)
b (Å)	3.9719(1)	4.0186(1)	4.0359(3)
c (Å)	7.2049(3)	7.1946(3)	7.1850(6)
β (°)	121.655(2)	109.715(2)	104.162(3)
Volume (Å^3)	284.08(2)	245.11(2)	696.16(10)
Z	2	1	2
R_{int}	0.024	0.028	0.056
R_σ	0.032	0.021	0.048
θ_{max}(°)	53.88	34.98	35.10
R_1 (obs)	0.024	0.023	0.026
R_1 (all)	0.036	0.032	0.049
wR_2 (obs)	0.048	0.050	0.041
wR_2 (all)	0.051	0.056	0.049
GooF	1.20	1.51	1.00
Δe (e/Å^3)	+1.9/−2.5	+3.9/−1.7	+1.7/−1.7

Rietveld refinements of the X-ray powder patterns (Figure 1) of mC-$La_2MnSe_2O_2$ and $La_6MnSe_4O_6$ revealed small fractions of impurity phases of ≈1% MnSe or ≈4% La_2SeO_2, respectively. The $La_4MnSe_3O_4$ sample contained a minor impurity phase (peak at $2\theta \approx 31°$) which has not been identified.

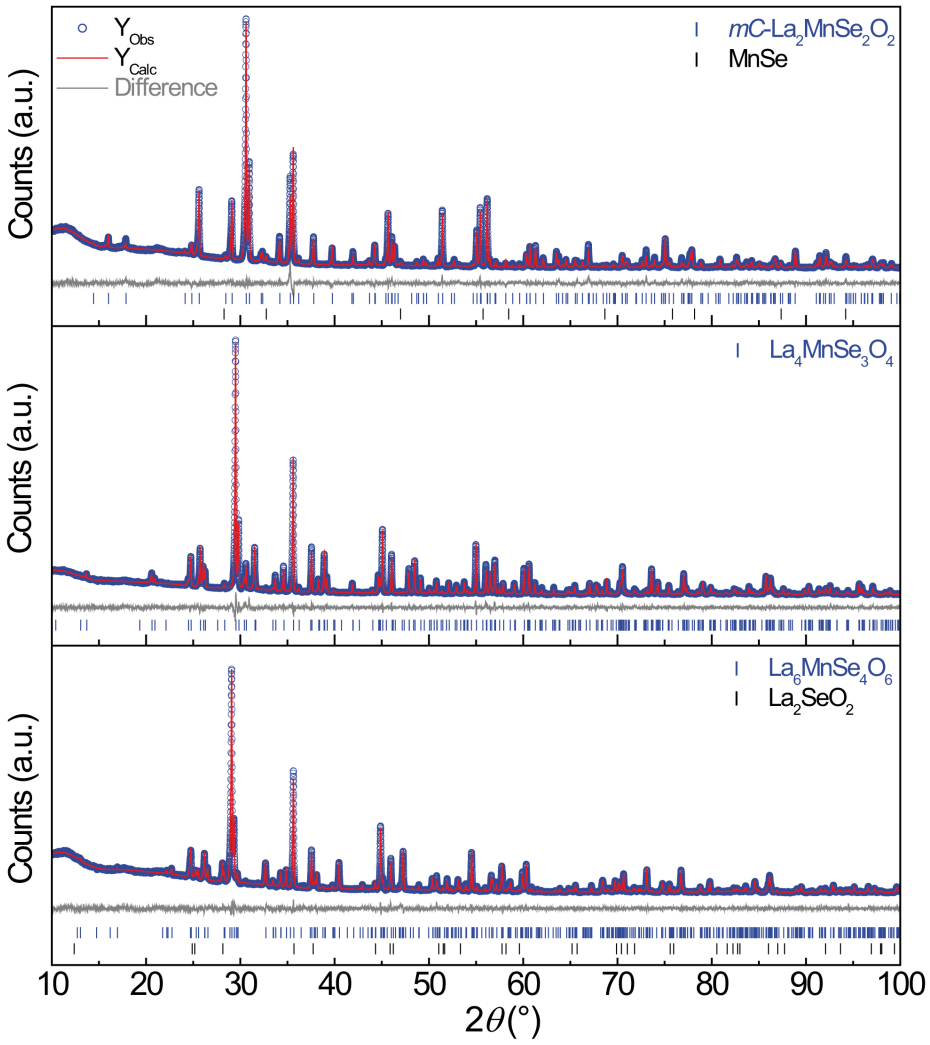

Figure 1. X-ray powder patterns (blue), Rietveld fits (red) and difference curve (gray) of *mC*-$La_2MnSe_2O_2$ (**top**), $La_4MnSe_3O_4$ (**middle**) and $La_6MnSe_4O_6$ (**bottom**).

2.1. *mC-La2MnSe2O2*

mC-$La_2MnSe_2O_2$ crystallizes isotypic with *mC*-$La_2FeSe_2O_2$ and *mC*-$Ce_2FeSe_2O_2$ [2] in the $Pb_2HgCl_2O_2$-type structure. The iron compounds are low-temperature polymorphs in the $RE_2FeSe_2O_2$ family (dwelling temperature = 1073 K), while *mC*-$La_2MnSe_2O_2$ is observed at high temperatures ($\geq$1273 K). The structure of *mC*-$La_2MnSe_2O_2$ consists of chains of distorted edge-sharing $MnSe_4O_2$-octahedra along the *b*-axis which are linked together along the *a*-axis by edge-sharing OLa_3Mn-tetrahedra forming infinite ribbons parallel to *b* (Figure 2). The La^{3+} ion has a distorted $LaSe_5O_3$ square antiprismatic coordination environment (Figure 3), which was already observed in $RE_4TiSe_4O_4$ compounds [13,14]. Similar to all $RE_2FeSe_2O_2$ polymorphs, the displacement ellipsoid of the manganese atom in *mC*-$La_2MnSe_2O_2$ exhibits an oblate spheroid shape in direction of the selenium atoms which is a consequence of the distorted $MnSe_4O_2$-octahedra. The distance between two manganese atoms in the $MnSe_4O_2$ chains (d_{intra}) is 397.2(1) pm, whereas the distance between the chains (d_{inter}) is 616.0(1) pm. Mn–O and Mn–Se bond lengths are 205.4(1) and 284.1(1) pm, respectively, which shows that $MnSe_4O_2$-octahedra are strongly compressed towards the oxygen atoms. The O–Mn–Se and Se–Mn–Se bond angles within the $MnSe_4O_2$-octahedra are nearly regular (88.7(1)°–91.3(1)°), while the La–O–La and La–O–Mn bond angles in the OLa_3Mn-tetrahedra are 105.1(1)°–115.8(1)° and thus differ significantly from a perfect tetrahedral shape (109.5°).

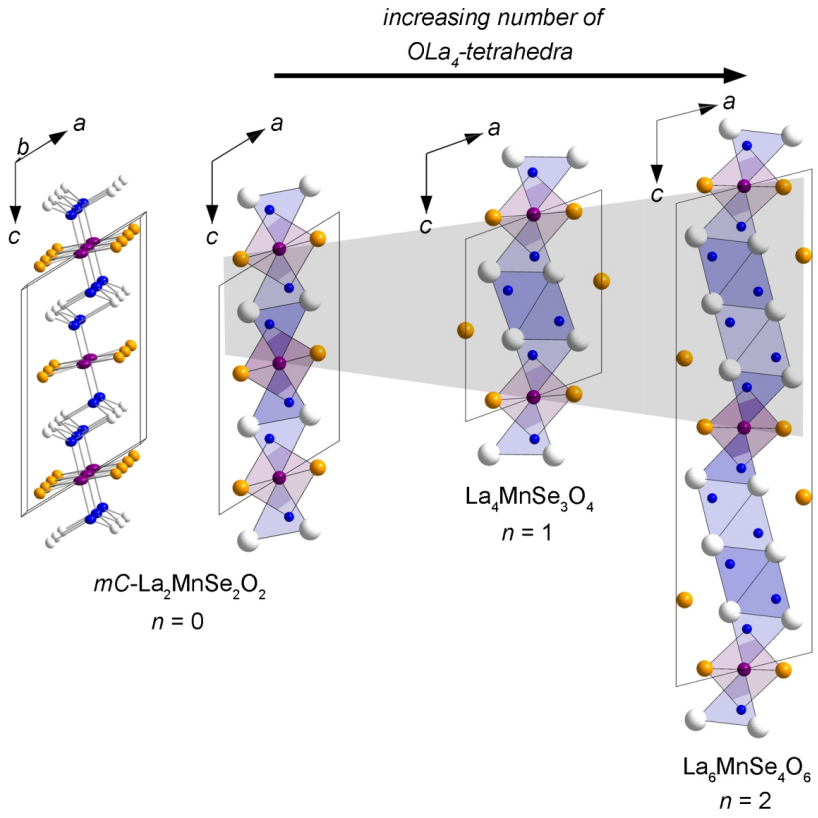

Figure 2. Crystal structures of $La_{2n+2}MnSe_{n+2}O_{2n+2}$ (n = 0–2). OLa_4- and OLa_3Mn-tetrahedra in blue, $MnSe_4O_2$-octahedra in violet. Rare-earth in white, manganese in violet, selenium in orange and oxygen in blue.

2.2. $La_4MnSe_3O_4$ and $La_6MnSe_4O_6$

$La_4MnSe_3O_4$ and $La_6MnSe_4O_6$ crystallize in new structure types which contain two or three crystallographically independent La atoms with two different coordination environments, respectively. The crystal structures are closely related to that of mC-$La_2MnSe_2O_2$ (Figure 2). They also consist of chains of edge-sharing $MnSe_4O_2$-octahedra along the b-axis. However, these octahedra are connected by two edge-sharing OLa_3Mn- as well as either two or four additional OLa_4-tetrahedra along the a-axis, respectively. The framework of four units wide, edge-sharing tetrahedra forming infinite ribbons was already observed in $RE_4TiSe_4O_4$ [13,14] and oP/oA-$La_2TSe_2O_2$ (T = Fe, Mn) [8]. Frameworks with six units wide tetrahedra are, to our best knowledge, unknown so far. $La_4MnSe_3O_4$ has two crystallographically independent La^{3+} ions which have either a La(1) Se_5O_3 square antiprismatic or a La(2) Se_3O_4 monocapped trigonal antiprismatic coordination environment. $La_6MnSe_4O_6$ contains a third independent La^{3+} ion which shows also a monocapped trigonal antiprismatic coordination. A comparison of the coordination evironments of the different lanthanum ions is depicted in Figure 3. The coordination polyhedra of La(1) and La(2) as well as La(2) and La(3) are connected via common Se–O edges. Compared to mC-$La_2MnSe_2O_2$, d_{intra} is slightly and d_{inter} is significantly longer in $La_4MnSe_3O_4$ and $La_6MnSe_4O_6$ as depicted in Table 2.

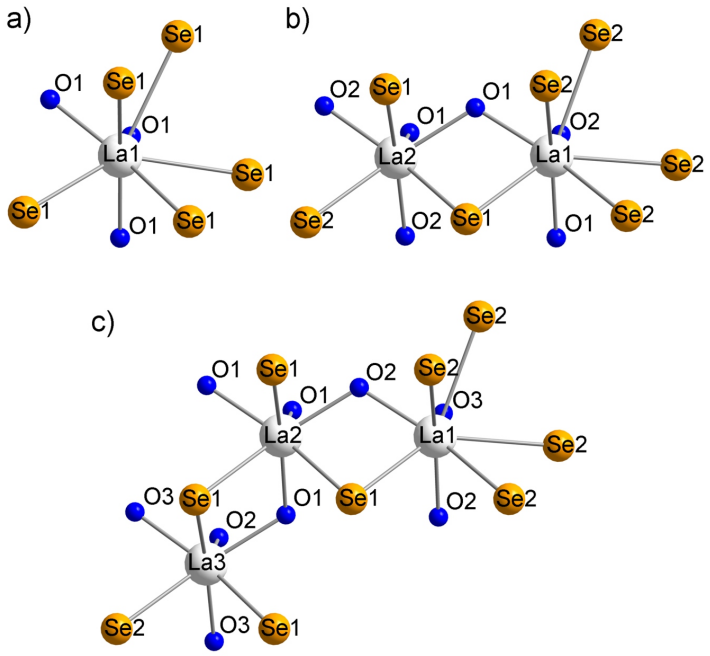

Figure 3. Coordination environments of the lanthanum ions in (**a**) *mC*-$La_2MnSe_2O_2$; (**b**) $La_4MnSe_3O_4$ and (**c**) $La_6MnSe_4O_6$ showing the connectivity between the distorted square and the mono-capped trigonal antiprisms.

Table 2. Distances between the manganese atoms in (d_{intra}) and between (d_{inter}) the $MnSe_4O_2$-octahedra chains and selected bond lengths (/pm) of *mC*-$La_2MnSe_2O_2$ (n = 0), $La_4MnSe_3O_4$ (n = 1) and $La_6MnSe_4O_6$ (n = 2).

n	d_{intra}	d_{inter}	d(Mn–O)	d(Mn–Se)	d(La–O)	d(La–Se)
0	397.2(1)	616.0(1)	205.4(1)	284.1(1)	234.4(1)–240.8(1)	315.9(1)–337.1(1)
1	401.9(1)	900.6(1)	207.0(1)	284.8(1)	236.4(1)–246.5(1)	313.0(1)–333.8(1)
2	403.6(1)	1247.8(2)	207.7(1)	284.8(1)	236.2(1)–245.2(1)	309.4(1)–333.3(1)

Selected bond lengths of the three members of the homologous series are depicted in Table 2. The Mn–O, Mn–Se and La–O bond lengths of $La_4MnSe_3O_4$ and $La_6MnSe_4O_6$ are very similar leading to strongly compressed $MnSe_4O_2$-octahedra analogue to those in *mC*-$La_2MnSe_2O_2$. As observed in *mC*-$La_2MnSe_2O_2$, the octahedra in $La_4MnSe_3O_4$ and $La_6MnSe_4O_6$ are more regular than the tetrahedra with respect to the bond angles listed in Table 3.

Table 3. Selected bond angles (°) of *mC*-$La_2MnSe_2O_2$ (n = 0), $La_4MnSe_3O_4$ (n = 1) and $La_6MnSe_4O_6$ (n = 2).

n	∠(La–O–La)	∠(La–O–Mn)	∠(Se–Mn–Se)	∠(Se–Mn–O)
0	105.1(1)–115.8(1)	106.4(1)–111.7(1)	88.7(1)–91.3(1)	89.5(1)–90.5(1)
1	102.8(1)–116.4(1)	106.9(1)–109.8(1)	89.8(1)–90.2(1)	87.8(1)–92.2(1)
2	102.8(1)–117.3(1)	106.0(1)–109.9(1)	89.8(1)–90.2(1)	88.0(1)–92.0(1)

2.3. Magnetism

The magnetic susceptibilities of *mC*-$La_2MnSe_2O_2$, $La_4MnSe_3O_4$ and $La_6MnSe_4O_6$ (Figure 4) obey the Curie–Weiss rule and indicate antiferromagnetic ordering of the moments near 15 K, similar to the Néel temperature of *mC*-$La_2FeSe_2O_2$ (T_N = 20 K, [2]). In case of *mC*-$La_2MnSe_2O_2$ and $La_4MnSe_3O_4$, χ_{mol} decreases clearly below this temperature, whereas the effect is more distinctive

for *mC*-$La_2MnSe_2O_2$. In contrast, the susceptibility of $La_6MnSe_4O_6$ shows no decrease in χ_{mol} but a clear turning point of the curve at this temperature.

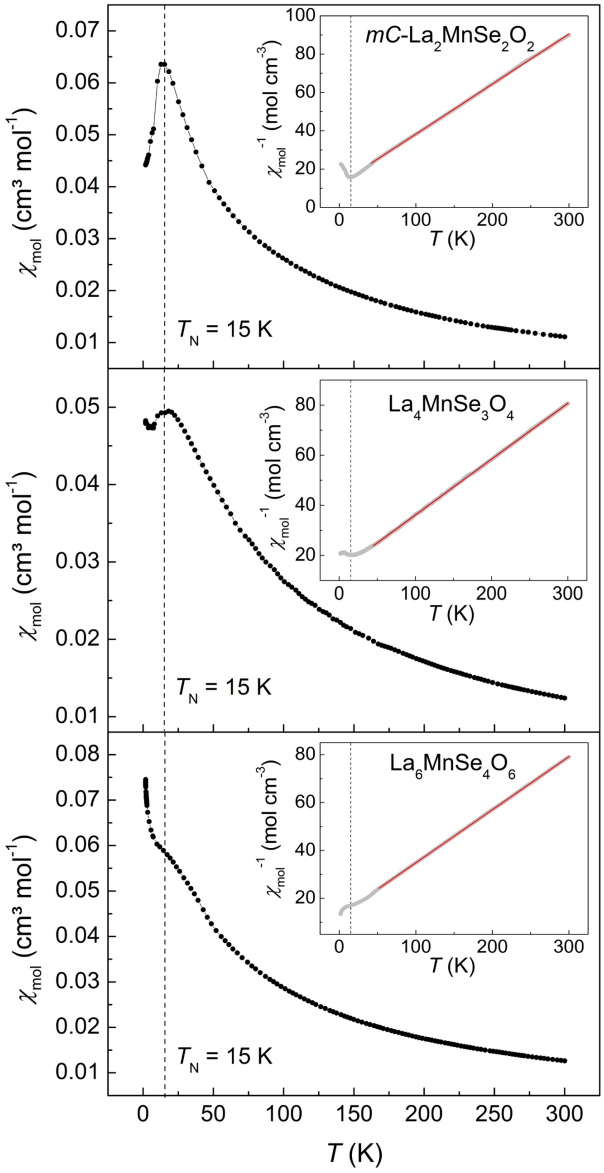

Figure 4. Magnetic susceptibilities (black, B = 1 T) and inverse susceptibilities (inset) of *mC*-$La_2MnSe_2O_2$ (**top**), $La_4MnSe_3O_4$ (**middle**) and $La_6MnSe_4O_6$ (**bottom**) with Curie–Weiss fit (red). Parameters obtained from the fits are given in Table 4.

Isothermal magnetization plots (see Figure A1 in the Appendix A) at 300 K are linear with field. *mC*-$La_2MnSe_2O_2$ exhibits a tiny hysteresis at 1.8 K, which can be due to small impurities, while those of $La_4MnSe_3O_4$ and $La_6MnSe_4O_6$ are nearly linear at 1.8 K. Plots of the inverse susceptibilities versus temperature (inserts in Figure 4) allow Curie–Weiss fits. The resulting effective magnetic moments (μ_{eff}) are 5.53(1), 5.98(1) and 6.01(1) μ_B per formula unit for n = 1, 2 and 3, respectively. Only the value for *mC*-$La_2MnSe_2O_2$ is slightly smaller than the theoretical moment of Mn^{2+} (5.92 μ_B). Negative values of the Weiss constant θ (Table 4) support antiferromagnetic ordering in all compounds.

Table 4. Effective magnetic moments (μ_{eff}), Weiss-constants (θ), and Curie-constants (C) of mC-$La_2MnSe_2O_2$, $La_4MnSe_3O_4$, and $La_6MnSe_4O_6$.

Compound	μ_{eff} (μ_B)	θ (K)	C ($cm^3 \cdot K \cdot mol^{-1}$)
mC-$La_2MnSe_2O_2$	5.53(1)	−46.5(1)	3.82(1)
$La_4MnSe_3O_4$	5.99(1)	−62.1(1)	4.48(1)
$La_6MnSe_4O_6$	6.01(1)	−57.4(1)	4.51(1)

The detailed magnetic structure is not ascertainable from susceptibilty data. We have recently determined the spin structure of $La_2CrSe_2O_2$ which is isotypic to mC-$La_2MnSe_2O_2$. Neutron powder diffraction [16] experiments revealed a three-dimensional (G-type) ordering, tantamount to antiferromagnetic order within and between the chains of $CrSe_4O_2$-octahedra. mC-$La_2MnSe_2O_2$ has presumably the same magnetic structure, and the almost identical Néel temperatures suggest at least similar magnetic ordering patterns in $La_4MnSe_3O_4$ and $La_6MnSe_4O_6$.

3. Materials and Methods

All starting materials (purity $\geq$ 99.9%) were handled in an argon-filled glove box (M. Braun, $p(O_2) \leq 1$ ppm, $p(H_2O) \leq 1$ ppm). Powder samples and single crystals of mC-$La_2MnSe_2O_2$ were prepared in a NaI/KI-flux starting from oC-$La_2MnSe_2O_2$, which was prepared as described in Reference [1]. oC-$La_2MnSe_2O_2$ (0.10 g) was sandwiched with 0.30 g of an eutectic mixture of NaI/KI (mass ratio 0.6:0.4, dried in dynamic vacuum at 673 K) in an alumina crucible. The crucible was sealed in an argon filled silica tube and heated to 1273 K at a rate of 100 K/h, kept at this temperature for 50 h and cooled to room temperature at a cooling rate of 100 K/h. Powder samples and single crystals of $La_4MnSe_3O_4$ and $La_6MnSe_4O_6$ were prepared in a two step reaction of appropriate amounts of La_2O_3, La_2Se_3 and MnSe. The rare-earth oxide was heated to 1273 K prior to use. La_2Se_3 was prepared by the reaction of freshly filed rare-earth metal and selenium powder at 573 K for 12 h. MnSe was prepared by the reaction of manganese and selenium powder at 1023 K for 24 h. The starting materials (0.20 g) were mixed intimately, filled in an alumina crucible, sealed in an argon filled silica tube and heated to 873 K at a rate of 25 K/h, kept at this temperature for 10 h and slowly cooled to room temperature at a cooling rate of 50 K/h. In a second step, the reaction mixture was ground in an agate mortar and sandwiched between 0.50 g of an eutectic mixture of NaI/KI. The crucibles were sealed in argon filled silica tubes and heated to 1073 K at a rate of 50 K/h, then to 1273–1373 K at a rate of 25 K/h, kept at this temperature for 40 h and cooled to room temperature at a cooling rate of 100 K/h. The reaction mixtures were then washed with deionized water and ethanol and dried in vacuum. The resulting samples were yellow-brown powders (purity > 95 wt %) and bright brown, transparent single crystals. The compounds are stable in air for months.

Single crystal X-ray diffraction data was collected with a Bruker D8 QUEST (fixed-χ goniometer, Mo-Kα, IμS with HE-LIOS multi-layer optics, PHOTON 100 detector, Bruker, Karlsruhe, Germany). Reflection intensity integration, data reductions, and multi-scan absorption corrections were done with APEX2 [17] and SADABS [18]. The structures were solved with Jana2006 [19]. Further details of the crystal structure investigations may be obtained from the Fachinformationszentrum Karlsruhe, 76344 Eggenstein-Leopoldshafen, Germany (Fax: +49-7247-808-666; E-Mail: crysdata@fiz-karlsruhe.de, http://www.fiz-karlsruhe.de/request for deposited data.html) on quoting the depository numbers CSD-432365 (mC-$La_2O_2MnSe_2$), CSD-432366 ($La_4MnSe_3O_4$) and CSD-432367 ($La_6MnSe_4O_6$).

X-ray powder diffraction patterns were measured with a Huber G670 diffractometer (Cu-Kα_1 radiation, Ge-monochromator, Huber Diffraktionstechnik GmbH & Co. KG, Rimstig, Germany). Rietveld refinements were done with TOPAS [20]. Magnetization isotherms and susceptibility measurements were performed with a MPMS-XL SQUID magnetometer (Quantum Design Inc., San Diego, CA, USA).

4. Conclusions

In this article we have reported the synthesis, structural characterization and magnetic properties of three new oxyselenides, which are members of the homologous series $La_{2n+2}MnSe_{n+2}O_{2n+2}$ (n = 0–2). The compounds are accessible using a flux synthesis at high temperatures (1273–1373 K). The crystal structures contain edge-sharing distorted $MnSe_4O_2$-octahedra along the *b*-axis as common building block. These are linked together along the *a*-axis by edge-sharing OLa_3Mn- and/or OLa_4-tetrahedra forming ribbons of increasing width. The lattice parameters *b* and *c* vary only slightly, whereas the monoclinic angle decreases strongly with increasing n. The magnetic susceptibilities obey the Curie–Weiss rule with effective magnetic moments compatible to Mn^{2+} and indicate antiferromagnetic ordering below 15 K.

Acknowledgments: We thank the German Research Foundation (DFG) for financial support.

Author Contributions: Simon Peschke and Dirk Johrendt equally contributed to the paper.

Conflicts of Interest: The authors declare no conflict of interest.

Appendix A

Table A1. Crystallographic data of *m*C-$La_2MnSe_2O_2$.

Formula weight (g·mol^{-1})	522.7
Space group, Z	$C2/m$, 2
a, b, c (Å)	11.662(1), 3.972(1), 7.205(1)
β (°)	121.7(1)
Volume (Å^3), $\rho_{X\text{-ray}}$ (g·cm^{-3})	284.1(1), 6.11
Crystal size (mm^3)	0.06 × 0.02 × 0.01
Diffractometer	Bruker D8 QUEST
Radiation λ (pm)	71.073
Absorption coeff. μ (mm^{-1})	29.6
2θ range (°)	6.64–107.76
Index range (*hkl*)	$-19 \leq h \leq 25$, $k \pm 8$, $-16 \leq l \leq 14$
No. reflections collected	5770
No. unique data, R_{int}, R_σ	1731, 0.02, 0.03
No. data with $I > 3\sigma(I)$	1441
No. parameters	23
R_1(obs/all)	0.024/0.036
wR_2(obs/all)	0.048/0.051
Δe (e/Å^3)	1.92/−2.53

Atomic and Displacement Parameters

	Site	x, y, z	U_{11}	U_{22}	U_{33}	Occ.
La	4*i*	0.6923(1), 0, 0.2430(1)	0.0073(1)	0.0058(1)	0.0059(1)	1
Mn	2*d*	0, $\frac{1}{2}$, $\frac{1}{2}$	0.0063(2)	0.0141(2)	0.0137(2)	1
Se	4*i*	0.9405(1), 0, 0.1797(1)	0.0087(1)	0.0088(1)	0.0080(1)	1
O	4*i*	0.8028(2), $\frac{1}{2}$, 0.4187(1)	0.0059(1)	0.0077(7)	0.0081(6)	1

Table A2. Crystallographic data of $La_4MnSe_3O_4$.

Formula weight ($g \cdot mol^{-1}$)	911.4
Space group, Z	$P2/m$, 1
a, b, c (Å)	9.006(1), 4.019(1), 7.195(1)
β (°)	109.7(1)
Volume (Å^3), $\rho_{X\text{-ray}}$ ($g \cdot cm^{-3}$)	245.1(1), 6.17
Crystal size (mm^3)	$0.04 \times 0.02 \times 0.01$
Diffractometer	Bruker D8 QUEST
Radiation λ (pm)	71.073
Absorption coeff. μ (mm^{-1})	29.4
2θ range (°)	4.80–69.96
Index range (hkl)	$h \pm 14$, $-6 \leq k \leq 5$, $l \pm 11$
No. reflections collected	6887
No. unique data, R_{int}, R_σ	1210, 0.03, 0.02
No. data with $I > 3\sigma(I)$	1017
No. parameters	39
R_1(obs/all)	0.023/0.032
wR_2(obs/all)	0.050/0.056
Δe (e/Å^3)	3.85/−1.71

Atomic and Displacement Parameters

	Site	x, y, z	U_{11}	U_{22}	U_{33}	Occ.
La1	2n	0.2245(1), $\frac{1}{2}$, 0.1732(1)	0.0053(1)	0.0056(1)	0.0046(1)	1
La2	2m	0.6430(1), 0, 0.3496(1)	0.0053(1)	0.0044(1)	0.0048(1)	1
Mn1	1f	0, $\frac{1}{2}$, $\frac{1}{2}$	0.0120(6)	0.0113(5)	0.0115(5)	1
Se1	1e	$\frac{1}{2}$, $\frac{1}{2}$, 0	0.0072(3)	0.0062(3)	0.0048(3)	1
Se2	2m	0.0627(1), 0, 0.7971(1)	0.0078(2)	0.0095(2)	0.0079(2)	1
O1	2m	0.3651(4), 0, 0.3114(5)	0.0048(16)	0.0069(16)	0.0082(16)	1
O2	2n	0.2317(4), $\frac{1}{2}$, 0.5070(5)	0.0046(16)	0.0057(15)	0.0079(16)	1

Table A3. Crystallographic data of $La_6MnSe_4O_6$.

Formula weight ($g \cdot mol^{-1}$)	1300.2
Space group, Z	$C2/m$, 2
a, b, c (Å)	24.760(1), 4.036(1), 7.185(1)
β (°)	104.2(1)
Volume (Å^3), $\rho_{X\text{-ray}}$ ($g \cdot cm^{-3}$)	696.2(1), 6.20
Crystal size (mm^3)	$0.03 \times 0.02 \times 0.01$
Diffractometer	Bruker D8 QUEST
Radiation λ (pm)	71.073
Absorption coeff. μ (mm^{-1})	29.3
2θ range (°)	5.84–70.20
Index range (hkl)	$-40 \leq h \leq 38$, $k \pm 6$, $l \pm 11$
No. reflections collected	8892
No. unique data, R_{int}, R_σ	1375, 0.05, 0.05
No. data with $I > 3\sigma(I)$	957
No. parameters	53
R_1(obs/all)	0.023/0.049
wR_2(obs/all)	0.041/0.049
Δe (e/Å^3)	1.65/−1.70

Atomic and Displacement Parameters

	Site	x, y, z	U_{11}	U_{22}	U_{33}	Occ.
La1	4i	0.0788(1), $\frac{1}{2}$, 0.1453(1)	0.0050(2)	0.0060(2)	0.0049(2)	1
La2	4i	0.2263(1), 0, 0.2665(1)	0.0045(2)	0.0044(2)	0.0043(2)	1
La3	4i	0.1261(1), 0, 0.6051(61)	0.0056(2)	0.0045(2)	0.0052(2)	1
Mn1	2d	0, $\frac{1}{2}$, $\frac{1}{2}$	0.0110(9)	0.0110(7)	0.0100(8)	1
Se1	4i	0.8252(1), $\frac{1}{2}$, 0.0613(1)	0.0069(3)	0.0067(3)	0.0048(3)	1
Se2	4i	0.4781(1), $\frac{1}{2}$, 0.2116(1)	0.0076(4)	0.0095(3)	0.0075(4)	1
O1	4i	0.2752(2), $\frac{1}{2}$, 0.3975(6)	0.004(2)	0.009(2)	0.006(2)	1
O2	4i	0.1288(2), 0, 0.2662(7)	0.007(2)	0.007(2)	0.007(2)	1
O3	4i	0.0823(2), $\frac{1}{2}$, 0.4801(6)	0.003(2)	0.005(2)	0.010(2)	1

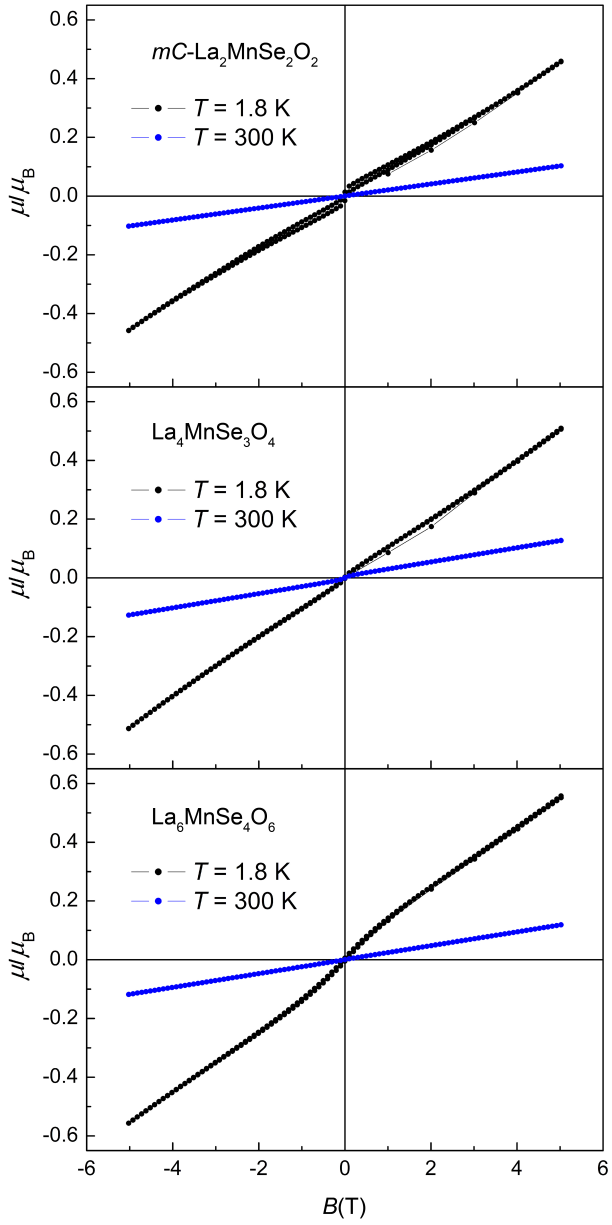

Figure A1. Isothermal magnetization plots at 300 K and 1.8 K of *mC*-$La_2MnSe_2O_2$ (**top**), $La_4MnSe_3O_4$ (**middle**) and $La_6MnSe_4O_6$ (**bottom**).

References

1. Peschke, S.; Nitsche, F.; Johrendt, D. Flux Synthesis, Modulated Crystal Structures, and Physical Properties of *RE*$Mn_{0.5}SeO$ (*RE* = La, Ce). *Z. Anorg. Allg. Chem.* **2015**, *641*, 529–536.
2. Nitsche, F.; Niklaus, R.; Johrendt, D. New Polymorphs of $RE_2FeSe_2O_2$ (*RE* = La, Ce). *Z. Anorg. Allg. Chem.* **2014**, *640*, 2897–2902.
3. Wang, C.H.; Ainsworth, C.M.; Gui, D.Y.; McCabe, E.E.; Tucker, M.G.; Evans, I.R.; Evans, J.S.O. Infinitely Adaptive Transition Metal Oxychalcogenides: The Modulated Structures of $Ce_2O_2MnSe_2$ and $(Ce_{0.78}La_{0.22})_2O_2MnSe_2$. *Chem. Mater.* **2015**, *27*, 3121–3134.
4. McCabe, E.E.; Free, D.G.; Evans, J.S.O. A new iron oxyselenide $Ce_2O_2FeSe_2$: Synthesis and characterisation. *Chem. Commun.* **2011**, *47*, 1261–1263.
5. Tuxworth, A.J.; McCabe, E.E.; Free, D.G.; Clark, S.J.; Evans, J.S.O. Structural Characterization and Physical Properties of the New Transition Metal Oxyselenide $La_2O_2ZnSe_2$. *Inorg. Chem.* **2013**, *52*, 2078–2085.

6. Ainsworth, C.M.; Wang, C.H.; Tucker, M.G.; Evans, J.S.O. Synthesis, Structural Characterization, and Physical Properties of the New Transition Metal Oxyselenide $Ce_2O_2ZnSe_2$. *Inorg. Chem.* **2015**, *54*, 1563–1571.
7. Hiramatsu, H.; Ueda, K.; Kamiya, T.; Ohta, H.; Hirano, M.; Hosono, H. Synthesis of single-phase layered oxychalcogenide $La_2CdO_2Se_2$: Crystal structure, optical and electrical properties. *J. Mater. Chem.* **2004**, *14*, 2946–2950.
8. McCabe, E.E.; Free, D.G.; Mendis, B.G.; Higgins, J.S.; Evans, J.S.O. Preparation, Characterization, and Structural Phase Transitions in a New Family of Semiconducting Transition Metal Oxychalcogenides β-$La_2O_2MSe_2$ (M = Mn, Fe). *Chem. Mater.* **2010**, *22*, 6171–6182.
9. Ainsworth, C.M.; Wang, C.H.; Johnston, H.E.; McCabe, E.E.; Tucker, M.G.; Brand, H.E.A.; Evans, J.S.O. Infinitely Adaptive Transition-Metal Ordering in $Ln_2O_2MSe_2$-Type Oxychalcogenides. *Inorg. Chem.* **2015**, *54*, 7230–7238.
10. Tougait, O.; Ibers, J.A. Synthesis and Characterization of Three New Rare-Earth Titanium Oxyselenides: $Ln_{3.67}Ti_2O_3Se_6$ (Ln = Ce, Nd, Sm). *Chem. Mater.* **2000**, *12*, 2653–2658.
11. Tougait, O.; Ibers, J.A. Syntheses and Crystal Structures of the Lanthanum Titanium Oxyselenides $La_4Ti_2O_4Se_5$ and $La_6Ti_3O_5Se_9$. *J. Solid State Chem.* **2001**, *157*, 289–295.
12. Dung, N.H.; Tien, V.V. Synthèse et structure cristalline d'une nouvelle famille d'oxyséléniures de chrome III et de lanthanides légers, de formule générale $RCrSe_2O$ (R= La, Ce). *C. R. Seances Acad. Sci.* **1981**, *293*, 933–936.
13. Meerschaut, A.; Lafond, A.; Meignen, V.; Deudon, C. Crystal Structure and Magnetic Properties of a New Oxyselenide of Gadolinium and Titanium: $Gd_4TiSe_4O_4$. *J. Solid State Chem.* **2001**, *162*, 182–187.
14. Tuxworth, A.J.; Evans, J. Synthesis, structure and properties of the oxychalcogenide series $A_4O_4TiSe_4$ (A = Sm, Gd, Tb, Dy, Ho, Er and Y). *J. Solid State Chem.* **2014**, *210*, 188–194.
15. Strobel, S.; Choudhury, A.; Dorhout, P.K.; Lipp, C.; Schleid, T. Rare-Earth Metal(III) Oxide Selenides $M_4O_4Se[Se_2]$ (M = La, Ce, Pr, Nd, Sm) with Discrete Diselenide Units: Crystal Structures, Magnetic Frustration, and Other Properties. *Inorg. Chem.* **2008**, *47*, 4936–4944.
16. Peschke, S.; Weippert, V.; Senyshyn, A.; Mühlbauer, M.J.; Janka, O.; Pöttgen, R.; Holenstein, S.; Luetkens, H.; Johrendt, D. Flux synthesis, crystal structures, and magnetic ordering of the rare-earth chromium(II) oxyselenides $RE_2CrSe_2O_2$ (RE = La–Nd). *Inorg. Chem.* **2017**, in press.
17. *APEX*2, version 2012.12-0; Bruker AXS Inc.: Madison, WI, USA, 2007.
18. Sheldrick, G.M. *SADABS*, version 2012/1; Bruker AXS Inc.: Madison, WI, USA, 2001.
19. Petricek, V.; Dusek, M.; Palatinus, L. *Jana2006*, version 26/09/2012; Institute of Physics: Praha, Czech Republic, 2006.
20. Coelho, A. *TOPAS-Academic*, version 4.1; Coelho Software: Brisbane, Australia, 2007.